Oral Presentation

The 7th TSME International Conference on Mechanical Engineering
13-16 December 2016

CST0016

Numerical investigation of an influence of square cylinder crossovers on twin bare hulls in close proximity

Pareecha Rattanasiri[1,*] and Philip A. Wilson[2]

[1] Department of Mechanical Engineering, Faculty of Engineering, Burapha University, Chon Buri Campus, Chon Buri, 20130, Thailand
[2] Fluid Structure Interactions Group, Faculty of Engineering and the Environment, University of Southampton, SO16 7QF, United Kingdom
[*] Corresponding Author: pareecha@eng.buu.ac.th, +66(0)9-2768-7904, Fax +66(0)3839-0351

Abstract

This paper investigates the influence of two crossovers on twin bare spheroids in close proximity. Firstly, to examine the impact of the crossovers to the flow behaviour and overall drag coefficient of spheroids. Secondly, to compare the drag coefficient for various speeds. The CFD RANS-SST with a commercial code ANSYS CFX simulation is performed for the fully submerged twin spheroids with transverse separation (*S/D*) of 1.02; where *S* is the distance between centreline to centreline and *D* is the maximum diameter of a spheroid. The Reynolds Numbers used are 2×10^6, 3×10^6, and 4×10^6. The results show that each spheroids experience an additional 20% drag which is dominated by crossovers. The drag coefficient of small volume crossovers between spheroids is 10 times higher than the drag of each spheroids, consequently, the total drag of system is increased by 11 times compares to twin bare spheroids system. Increasing speed results in the drag reduction. At the Reynolds Number 2×10^6 shows the highest drag coefficient of twin hulls for both cases (with or without crossovers). The result suggests the use of twin bare hulls without crossovers in the fleet, an application; for example, a fleet of small autonomous underwater vehicles.

Keywords*:* spheroid drag, flat plate drag, fully-submerged hulls, RANS-SST, ANSYS CFX

1. Introduction

Rattanasiri *et al*. [1] found that the close proximity distance between parallel-twin self-propelled AUVs increases the resistance of each hulls and the overall drag of the fleet. Rattanasiri *et al*. [2] reported that the distance between twin bare hulls which is less than 3D could result in individual drags and overall drag increments. Where D is the maximum diameter of hull. To maintain the distance of both hulls, adding square crossovers in between could be one of an options. Therefore, the simulation of fully-submerged twin hulls with crossover plates will be performed in this study by using CFD RANS-SST with a commercial code ANSYS CFX. The aim is to investigate the influence of square crossovers. To achieve this aim, two hydrodynamic processes of twin bare hulls: the body-to-body interference (or viscous interaction) and drag increment due to an additional crossover plate would be numerically investigated.

The purpose of this paper is to provide guidance for AUV's designers of multiple vehicles operated in a fleet on different Reynolds Number.

2. Theoretical approach

By assuming the hulls are fully submerged in deep water, there will be no wave resistance ($C_{wave} \approx 0$). Theoretically, the total drag coefficient (C_D) for fluid flow passes twin hulls in parallel configuration could therefore due to the viscous drag (C_v) only:-

$$C_D = C_{wave} + C_v \approx C_v$$

Thus $$C_D \approx C_v = (1 + k)C_F \qquad (1)$$

Where $(1 + k)$ is a form factor and C_F is the skin friction drag which could be estimated by [3]:-

$$C_F = 0.075/(log_{10}(Re) - 2)^2 \qquad (2)$$

For a single hull with streamlined shapes, an estimated form factor in terms of the body length (L) and the maximum body diameter (D) is [4]:-

$$(1 + k) = 1 + 1.5(D/L)^{3/2} + 7(D/L)^3 \qquad (3)$$

In the case of parallel twin hulls in close proximity, the conventional form factor for a single hull cannot establish an accurate prediction due to the accelerated flow velocity between the twin hulls as shown in Figure 1. This is termed a viscous interaction effect (1+*Bk*), which results in an increase of the drag of both hulls [1][2].

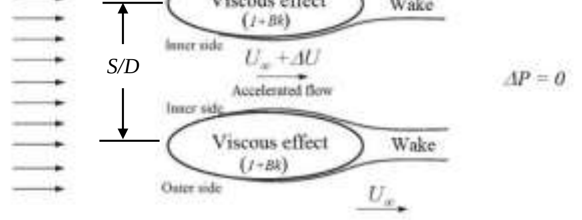

Figure 1: Flow past twin hulls in parallel configuration

Otherwise, physically, the components of hydrodynamic drag coefficient (C_D) acting on a hull are pressure drag coefficient (C_P) and skin friction drag coefficient (C_F).

$$C_D = C_P + C_F \quad (4)$$

To predict these hydrodynamic drags, a steady-state Reynolds Averaged Navier Stokes (RANS) simulation has proved to provide reasonably accurate results with a viscous interaction effect (1+*Bk*) when compared against the experimental results [1][2][5][6]. The CFD-RANS simulation with a commercial code ANSYS CFX [9] is then selected. The drag coefficient of hull could then be estimated by:-

$$C_D = (\text{Total drag})/\ (0.5\ \rho\ V^2 A_w) \quad (5)$$

Where ρ is the fluid density, A_w is the hull's wetted surface area and V is the vehicle speed.

By assuming the flow is incompressible, the continuity equation becomes:-

$$\frac{\partial \overline{U_i}}{\partial x_i} = 0 \quad (2)$$

The momentum equation can be written as:-

$$\rho\left(\frac{\partial \overline{U_i}}{\partial t} + \frac{\partial \overline{U_i U_j}}{\partial x_j}\right) = -\frac{\partial \bar{P}}{\partial x_i} + \frac{\partial}{\partial x_j}\left\{\mu\left(\frac{\partial \bar{U}_i}{\partial x_j} + \frac{\partial \bar{U}_j}{\partial x_i}\right)\right\} - \rho\frac{\partial \overline{u_i' u_j'}}{\partial x_j} + \bar{f_i} \quad (3)$$

where the tensor x_i represents Cartesian co-ordinates (*X*, *Y*, *Z*) and U_i are the Cartesian mean velocity components (U_x, U_y, U_z). The Reynolds stress tensor ($\rho u_i' u_j'$) is represented in the turbulence closure and $\bar{f_i}$ is the external forces. The previous investigations [1][2][6] have shown that the shear stress transport (SST) turbulence closure model (which blends $k-\varepsilon$ and $k-\omega$) is better able to replicate the flow around hull forms than either $k-\varepsilon$ or $k-\omega$ model, notably with a moderate computer accuracy [1][2][7][8]. Therefore, SST turbulence model was selected. However, to obtain a high fidelity simulation result needs an appropriate mesh strategy and mesh resolution to capture the effect of the boundary layer, body-to-body interaction and the wake behind the body [1][2], therefore, it is important to introduce the mesh strategy used in the next topic.

3. Case study

3.1 Base Experiment

Molland and Utama [6] investigated the side-force and yawing moment interactions between a pair of prolate spheroids in the 7' × 5' (2.20 m × 1.57 m) low speed wind tunnel at the University of Southampton. The top spheroid (B1) was fitted to the overhead wind tunnel dynamometer for measuring the total drag and side-force. It was placed at the middle breadth and 1.07 m height from the floor. The lower spheroid (B2) was placed at various transverse separation (*S*/*D*). The noses of both spheroids are aligned with zero longitudinal offset as shown in Figure 1. By using equations (1) to (3), the experimental drag of a single hull [6] could be calculated.

Rattanasiri *et al.* [2] performed a set of CFD simulation to compare with experimental results [6]. The simulation results of a single hull exhibited good correlation with the pressure distribution, the side-force coefficient, form factor and the drag in [6]. This numerical setting and the mesh strategy [2] have proved to provide a good agreement of total drag between the simulation results [2] and the experimental results [6] and the empirical results [4]. Thus, by modelling flat plates into this twin hulls simulation model [2], the investigation of the impact of crossover to a fleet of twin hulls can be performed with a degree of certainty.

3.2 Present study

The previous simulation in 3.1 is performed for a pair of twin hulls aligned with zero longitudinal offset at *S*/*D* = 1.02 (Figure 2), it would be used as the benchmark case for this study. Simulations are then performed for twin hulls with square crossover in Figure 3.

3.2.1 Hulls, model domain and boundary condition

Each hull is modelled by a shape profile of prolate spheroid 6:1 (1.2 m long with maximum diameter 0.2 m). The wet surface area (A_w) is 0.601 m^2. The square cylinder shape has the thickness of 10% of spheroid's diameter.

The dimension of fluid domain is modelled as 1.4*L* × 12*L* × 1.8*L*. Free slip wall conditions are used for the roof, floor and walls. The water inlet velocity (*V*) is set at 2.058 m/s, 3.08 m/s and 4.0 m/s related to the Reynolds Number of interest are at 2×10^6, 3×10^6, and 4×10^6 for a fully submerged case, with the zero relative pressure outlet boundary condition. Both hulls are modelled by using no slip wall condition. See Figure 5.

3.2.2 Mesh strategy

Sample of meshing shows in Figure 6 and 7. The computational parameters are provided in Table 1 and Table 2. See the references [1] and [2] for more detail of mesh strategy and mesh validations.

Table 1: Computational parameters

Parameters	Setting
Mesh type	Unstructured with local refinement around spheroids and in wake regions
y+	average 30
No. of elements	3-40 Millions with 15 prism layers in the boundary layer
Turbulence model	Shear Stress Transport
Inlet turbulent intensity	1%
Wall modelling	Automatic Wall Function
Spatial discretisation	High Resolution
Timescale control	Auto Timescale
Convergence criteria	RMS residual < 10^{-6} for bare hulls RMS residual < 10^{-4} for hulls with crossovers
Run type	Parallel run on 4×Dual core nodes, each with 2GB RAM

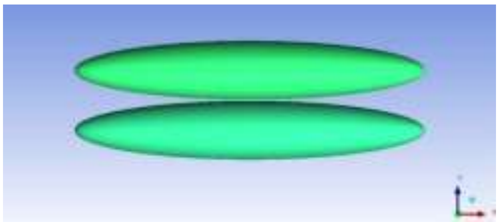

Figure 2: Top view (ZX plane) of twin towed hulls

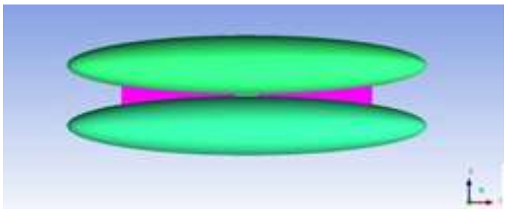

(a) Top view (ZX plane) of hulls with crossover

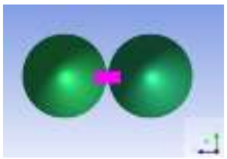

(b) Front view (YZ plane) of hulls with crossover

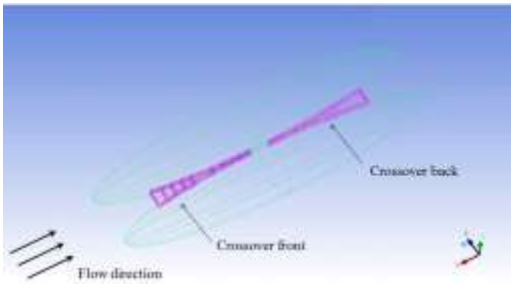

(c) Isometric view of hulls with crossover

Figure 3: Towed hulls with square crossovers

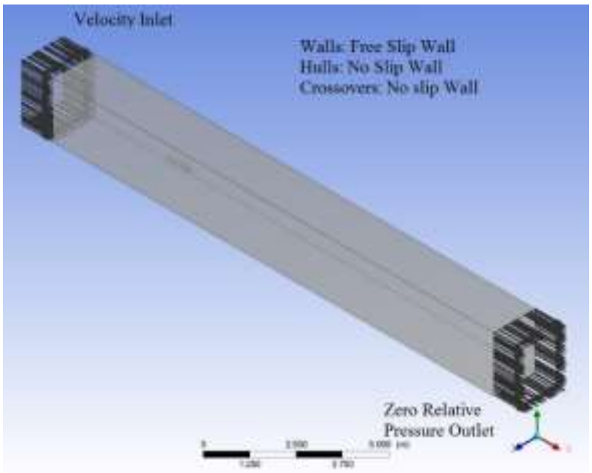

Figure 4: Fluid domain and boundary condition

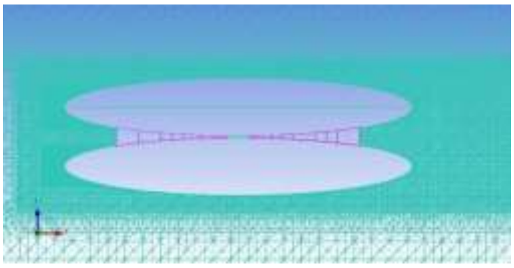

Figure 5: Fine mesh set on ZX plane at $Y = 0$ from the centreline with the fluid flow from left to right

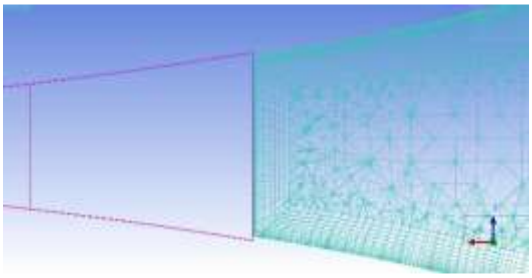

(a) ZX plane at $Y = 0$ m from the centerline

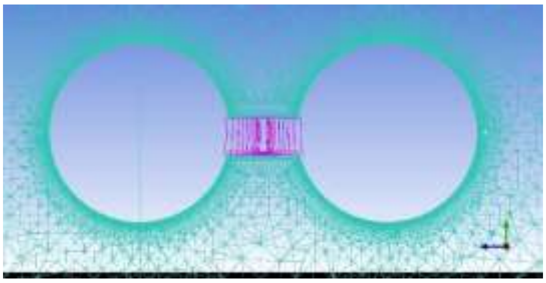

(b) YZ plane at $X = 1.0$ m from the noses

Figure 6: Prism layers of mesh cut around a pair of spheroids for coarse mesh

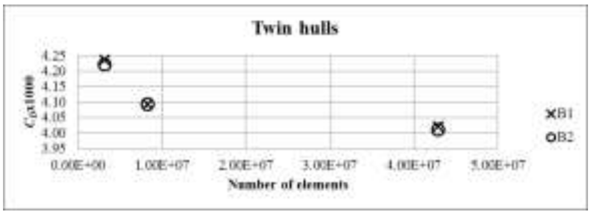

Figure 7: Mesh convergence

Table 2: Mesh strategies

meshing	No. of Nodes	No. of elements	Mesh differences	Simulation time (wall clock hours)
Coarse	1275256	3216827	-	2.5
Medium	2144354	8337793	5120966	6
Fine	8366608	42903041	34565248	48

CST0016

4. Result

4.1 Mesh convergences

One measure of accuracy of the numerics is the effect of mesh convergence. Mesh convergences were tested as the results shown in Figure 7. Definition of $\%C_{D(B1)}$ and $\%C_{D(B2)}$ are as following;

$$\%C_{D(B1)} = \frac{C_{D(B1,i)} - C_{D(B1,i-1)}}{C_{D(B1,i)}} \times 100,$$
$$\%C_{D(B2)} = \frac{C_{D(B2,i)} - C_{D(B2,i-1)}}{C_{D(B2,i)}} \times 100 \qquad (4)$$

where i is the drag coefficient of coarse, medium and fine mesh. Table 3 shows results of total drag coefficient (C_D), the skin friction drag coefficient (C_F) and the pressure drag coefficient (C_P). The results show the convergence of meshing from coarse, medium to fine mesh. From accuracy and time consuming prospect, the fine mesh set up is selected in this study.

4.2 Influence of flat plate crossovers to twin hulls

The samples of velocity contour of flow past twin hulls are shown in Figure 7. The contours show that the front crossover increases the velocity flow around hulls, overall the fluid domain and also accelerated the wake flow. Consequently, drag of both hulls is significantly increased by the higher viscous drag.

At 4 m/s, twin hulls with crossovers show an increase of drag approximately 21% and 19% higher than twin hulls without crossovers for B1 and B2, respectively. The results are dominated by the drag of the crossover front which is approximately 12 times of individual C_D of B1 (also B2).

4.3 Impact of the Reynolds number to individual hulls

C_D of B1 (also B2) is reduced about 11% for the speed of flow increased from 2.058 m/s to 4.0 m/s, while C_D of B1 (also B2) with crossover is reduced about 5% for flow speed increased from low to high. It shows that the crossover also influences the individual drag considering the different speed, while the increase of flow speed show no effect on the individual plate drag. The same results show for B2.

4.4 Impact of the Reynolds number to crossovers

The drag coefficient results show in Table 4. Increasing speed results in the drag reduction. The speed of 2.058 m/s shows the highest drag coefficient of twin hulls for both cases (with or without the crossover).

From Table 4, the front crossover experiences approximately 10 times higher drag than individual hulls' drag. Due to the pressure recovery, the back crossover experiences the drag reduction [2].

5. Conclusion and Suggestion

Due to the accelerated flow by the flat plate, the viscous effect is highly increased. Therefore, the crossovers flat plate shape could influence the increase of individual hull's drag by approximately 20%. The result also demonstrated the crossovers increase the drag of the overall vehicle's drag by 11 times of the twin hulls without crossovers.

Based on the information of C_D based shape frontal area [6], the change of front crossover shape from square cylinder to be half-cylinder could lead to the drag reduction of the front crossover by half [6] and could lead to slightly drag reduction of twin hulls with crossovers, however, still no benefit of using the crossovers considering overall drag reduction of vehicle to be suggested.

6. Acknowledgement

The authors acknowledge the use of the IRIDIS High Performance Computing Facility, and associated support services at the University of Southampton, in the completion of this work.

7. References

[1] Rattanasiri, P, Wilson P.A. and Phillips, A.B. (2014). Numerical Investigation of a fleet of towed AUVs. *Ocean Engineering*. vol 80C: pp. 25-35.

[2] Rattanasiri, P, Wilson P.A. and Phillips, A.B. (2013). Numerical Investigation of a pair of self-propelled AUVs operating in tandem. *Ocean Engineering*. vol. 100, pp 126-137.

[3] ITTC (1957). Proceeding of the 8th ITTC, Madrid, Spain. In: Canal de Experiencias Hidrodimanics, El Pardo, Madrid.

[4] Hoerner, S.F. (1965). Fluid-dynamic drag: practical information on aerodynamic drag and hydrodynamic resistance. (Published by the author).

[5] Phillips, A.B., Furlong, M. and Turnock, S.R. (2007). The use of computational fluid dynamics to assess the hull resistance of concept autonomous underwater vehicles. in OCEANS 2007 IEEE Aberdeen.

[6] Molland, A.F., and Utama, I.K.A.P. (1997) Wind tunnel investigation of a pair of ellipsoids in close proximity. Technical Report 98. Ship Science, University of Southampton.

[7] Larsson, L. and Baba, E. (1996). "Ship resistance and flow computations." Advances in marine hydrodynamics. vol 5. pp. 1–75. Computational Mechanics Publications.

[8] Phillips, A. B. (2010) Cost effective hydrodynamic concept design of autonomous underwater vehicles. PhD. Thesis. University of Southampton.

[9] ANSYS, 2010. ANSYS CFX, Release 12.1. ANSYS.

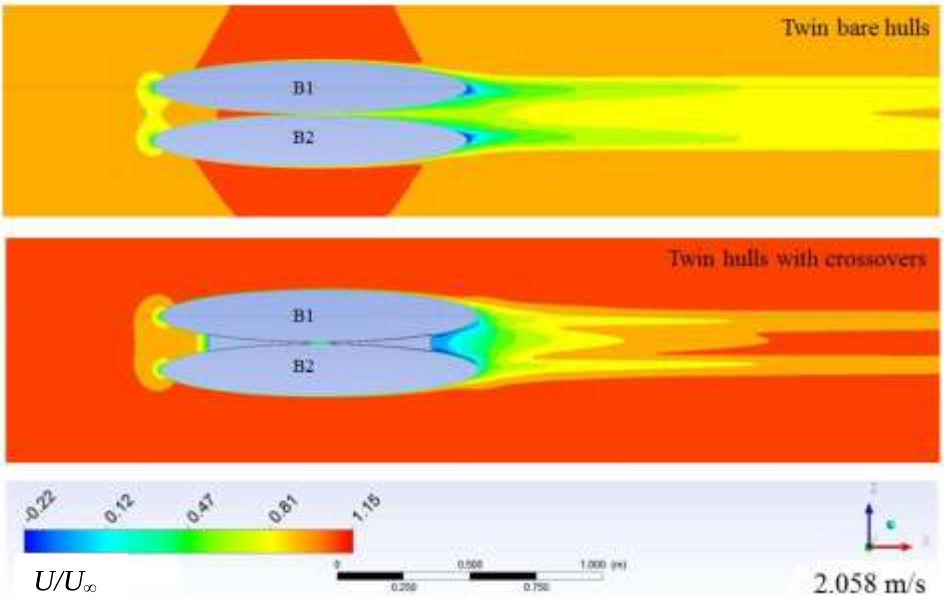

Figure 7: The velocity profile of 2.058 m/s flow past twin hulls with and without crossovers

Table 3: The drag coefficient, skin friction coefficient and pressure coefficient for speed of 4.0 m/s

	B1	B2	B1	B2	B1	B2	Eq. (4)	Eq. (4)
meshing	C_F ×1000	C_F ×1000	C_P ×1000	C_P ×1000	C_D ×1000	C_D ×1000	$\%C_{D(B1)}$	$\%C_{D(B2)}$
Coarse	3.5211	3.5174	0.7203	0.7100	4.2355	4.2220	-	-
Medium	3.5135	3.5105	0.5857	0.5871	4.0935	4.0923	3.47	3.07
Fine	3.5154	3.5119	0.5081	0.4998	4.0214	4.0101	1.79	2.05

Table 4: Comparison of the drag coefficient of twin bare hulls and twin hulls with square cylinder crossovers. Sign + is the drag increment and sign – is the drag reduction.

	Re × 10^{-6}	V (m/s)	B1	B2	B1	B2	B1	B2	Cross-over Front	Cross-over Back	Total Cross-over
			C_D ×1000	C_D ×1000	C_F ×1000	C_F ×1000	C_P ×1000	C_P ×1000	C_D ×1000	C_D ×1000	C_D ×1000
Twin bare hulls	**2**	2.058	4.528	4.516	3.934	3.931	0.596	0.587	-	-	-
	3	3.08	4.210	4.199	3.673	3.669	0.539	0.532	-	-	-
	4	4.0	4.021	4.010	3.515	3.512	0.508	0.500	-	-	-
Twin hulls with cross-overs	**2**	2.058	5.111	5.023	3.588	3.536	1.524	1.496	59.519	-3.665	55.854
	3	3.080	4.948	5.001	3.274	3.310	1.682	1.697	60.385	-5.448	54.938
	8	4.000	4.870	4.769	3.124	3.054	1.740	1.713	59.954	-5.922	54.032